

DESIGN AND DEVELOPMENT OF THE NEW DIAGNOSTICS CONTROL SYSTEM FOR THE SPES PROJECT AT INFN-LNL

G. Savarese*, G. Arena, D. Bortolato, F. Gelain, D. Marcato, V. Martinelli, E. Munaron, M. Roetta
INFN/LNL, Legnaro, PD, Italy

Abstract

The need to get finer data to describe the beam is a relevant topic for all laboratories. For the SPES project at Laboratori Nazionali di Legnaro (LNL) a new diagnostic control system with more performing hardware, with respect to the one used in legacy accelerators based on Versabus Module Eurocard (VME) ADCs, has been developed. The new system uses a custom hardware to acquire signals in real time. These data and ancillary operations are managed by a control system based on the Experimental Physics and Industrial Control System (EPICS) standard and shown to users on a Control System Studio (CSS) graphical user interface. The new system improves the basic functionalities, current read-back over Beam Profilers (BP) and Faraday Cups (FC) and handlings control, with new features such as: multiple hardware gain levels selection, broken wires correction through polynomial interpolation and roto-translations taking into account alignment parameters. Another important feature, integrated with the usage of a python Finite State Machine (FSM), is the capability to control an emittance meter to quickly acquire data and calculate beam longitudinal phase space through the scubeex method.

INTRODUCTION

The SPES project, acronym for Selective Production of Exotic Species, is the new leading project of the Legnaro National Laboratories (LNL) an Italian international center for the nuclear and astronuclear physics research. The objective of the SPES project is to study exotic beams made up of ions much more neutron-rich than those we can find in nature. It will exploit the legacy accelerator ALPI (Linear Accelerator for Ions) and will be employed as another ions source in parallel to the existing ones. [1] Since the beam will be post-accelerated in the ALPI accelerator, the beam line is made up of instruments aiming to optimize the beam transport, to reduce the energy spread, to clean the beam from undesired isobaric masses, to boost the beam charge and to pulse the beam. In a transport beam line the fundamental elements to monitor the beam shape, position and intensity are the diagnostics. They are essential to understand how to modify system parameters to obtain the desired beam [2].

The SPES project was the trampoline for the LNL to upgrade the hardware used to acquire and elaborate data and to adopt the Experimental Physics and Industrial Control System (EPICS) standard [3], that is a set of software tools developed to operate particle accelerators allowing information access and exchange between different subsystems. In fact a general upgrade of the legacy diagnostic control system

* giovanni.savarese@lnl.infn.it

was needed since the computer technologies improvement and the increasingly challenging accelerator data acquisition requested the design of a new modular and maintainable software and a hardware offering better performances.

This paper shows the most significant details and advantages of the new hardware configuration and the EPICS Input Output Controller (IOC) developed to communicate with the hardware components and the other subsystems already developed at the LNL.

THE LEGACY CONTROL SYSTEM

The legacy diagnostic control system is currently mounted in the ALPI and PIAVE (Positive Ions Accelerator for VEry low velocity ions) facilities and its target is to control and display details related to Faraday Cups (FC) and Beam Profilers (BP). Our FCs are copper cups used to collect and measure all the beam current; a metal shield, charged with high negative voltage, avoids that secondary electrons exit the cup. Our BPs are made up of two perpendicular grids (vertical and horizontal) with 40 parallel tungsten wires. Other diagnostic instruments are the collimators (or slits), used to narrow the beam, and the Emittance Meters (EM), which measures the longitudinal phase space and the energy spread.

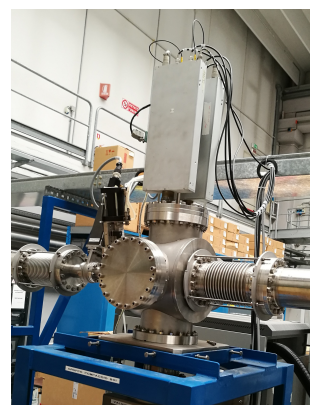


Figure 1: Diagnostic box with the legacy pre-amplifier grids.



Figure 2: VME Rack.



Figure 3: Legacy diagnostic GUI.

The electronics, for grids signals, is made up of an analog board, as shown in Fig. 1, mounted close to the detector to reduce the signal path. It has a current to voltage converter for each wire of the grid and a multiplexer system generates an output buffer to send to a Versabus Module Eurocard (VME) ADC board. The current amplification, performed by the converters, is controlled by two transistor-transistor logic (TTL) signals connected to two analog switches; the saturation levels are respectively 10 nA and 100 nA and the lower detectable current is 1 nA [4].

The VME ADC board, Fig. 2, is located outside the bunker to ease maintenance and reduce the exposure of electronic instrumentation to radiations. This board provides 12 bits resolution and supports a conversion rate of 100 KHz. Current signals coming from the FC are directly amplified and digitized. BP signals come as two buffers of 40 voltage signals and the board scans them thanks to a clock signal, composed by 40 TTL period pulses of 200 μ s each one, kept 1.6 ms apart. The clock signal and the selection gain signals pass through a digital buffer, suited to drive 50 Ω loads in a daisy-chaining arrangement through subsequent boxes.

At the beginning, the software layer was based on C programs developed on VxWorks Operating System (OS). Then it was replaced by a custom EPICS based control system, hosted by the VxWorks OS with a device driver realizing the interface between the field and the EPICS server host: the IOC receives the BPs and FCs digitized values and apply a software conversion to retrieve the current values [5].

The steppers motor controllers are VME cards built at the LNL, together with the associated power drivers: every single controller is able to manage up to 8 motors. The controller is VME based and is hosted, with the associated EPICS IOC, by a VxWorks OS.

A Control System Studio (CSS) Graphical User Interface (GUI), Fig. 3, has been developed to read the EPICS Process Variables (PVs). The main panel shows general information about diagnostic boxes, such as BPs and FCs status and commands. When selecting a specific diagnostic, users are redirected to a page showing the beam vertical and horizontal profile and the FC current. From the same page, it is possible to graphically adapt the signal full-scale, but not the hardware gain value, and to insert or extract the BP and the FC when presents.

CONTROL SYSTEM UPGRADE

The new control system will be EPICS based and will run on a Linux virtual machine instead of on an embedded OS. It will exploit a more performing hardware and an improved software with new features. Since the control system upgrade will take some time, and in an initial period there will be a mixed regime with both the old and the new control system, the requirements are: both hardware and software must be backward compatible with the exiting ones and modular; to improve the acquisition precision and the position control; possibility to hide broken wires, which usually falsify the measurement, and reorder switched wires; create

an improved GUI similar to the legacy one; integration of different type of handling systems.

Hardware

Knowing these requirements, we developed a custom multi input and output purposes controller and a pre-amplifier box [6].



Figure 4: Custom pre-amplifier box developed at LNL.



Figure 5: Custom controller developed at LNL.

In the new configuration, two 40 wires cables start from the same BP and reach the same pre-amplifier box, Fig. 4. They bring information about the vertical and horizontal profile each. The new pre-amplifier box is made up of two board, each with 40 Operational Amplifier (OA). Each OA converts the received current value into a voltage value in the range [-10, 10] V performing a signal amplification based on the selected gain. The selected gain is the same for all the OA in the box. There are 4 gain levels allowing to read current values from 1 pA up to 10 μ A. The converted signals, using the clock signal received from the controller, are then multiplexed over a single wire and forwarded to the controller. The new pre-amplifier box can be controlled by both the legacy VME board and the new controller.

To replace the legacy VME crates, we chose to use the controller in Fig. 5 which is a smarter and more cost-effective solution for those applications, not involved in high-reliability processes, where the control tasks are reduced to simple analog and digital I/O operations. The core element is the Field Programmable Gate Array (FPGA) allowing to perform real time tasks, fast peripherals control, data acquisition, digital data pre-processing and data buffering. The configurable digital and analog I/O channels and the external communication through gigabit Ethernet and Wi-Fi make the controller

a complete and improved data acquisition system for real time applications with respect to the legacy electronics. The I/O channels flexibility and the fact that the FPGA can be programmed to generate clock and gains signals, equal to the ones generated by the VME crates, makes the controller backward compatible allowing the communication with both the legacy analog boards and the new pre-amplifier boxes.

Thanks to its modularity, a single controller can manage up to 4 pre-amplifier boxes (equivalent to 4 BPs) and 4 FCs. BPs values arrive to the controller as two buffers of 40 voltage signals and an ADC digitizes them into two arrays of 16 bits values. The ideal conversion is expressed in Eq. (1). These arrays are stored in specific registers of the FPGA. On the other side, the controller uses a CAENels board to read FCs current values. The readable current range spans in the range $[-FS, FS]$, where FS stands for the hardware full-scale imposed by the selected gain which can be 1 mA or 1 μ A. The digitized value is saved as a 20 bits value in the FPGA register and Eq. (2) describes the ideal conversion.

$$X_{BP,i} = \frac{V_{BP,i} \cdot 2^{16}}{2 \cdot FS_{BP}} = V_{BP,i} \cdot G_{BP} = I_{BP,i} \cdot G_{PA,i} \cdot G_{BP} \quad (1)$$

$$X_{FC} = \frac{I_{FC} \cdot 2^{20}}{2 \cdot FS_{FC}} = I_{FC} \cdot G_{FC} \quad (2)$$

EPICS IOC

For the software development we chose to use the EPICS framework and we implemented a new IOC from scratch. The IOC reads the data saved in the controller's FPGA, elaborates those data and communicates with external IOCs controlling different types of handling systems. To provide a common interface, during the transaction phase where both the control systems will coexist, a software abstraction layer inside the new IOC communicates with the PVs of the legacy diagnostic IOC and integrates them in the new control system.

Current values retrieval To communicate with the controller, the IOC makes use of IPBUS. IPBUS is an IP-based communication protocol and the transport protocol can be UDP (User Datagram Protocol) or TCP (Transmission Control Protocol) based. At LNL we developed an EPICS device support to implement the IPBUS protocol based on UDP. Through this module we can associate a generic PV to specific FPGA memory register. This way PVs can access acquired data or can change the acquisition mode changing the related control bits. Thanks to these control bits, users can select the gain to apply during the acquisition.

Once the IOC has loaded the raw values, knowing the hardware specifications and given a set of calibration values to compensate the ADC and OA errors, the logic retrieves the correct current value. For BPs, the controller acquires array of values, so the conversion and the calibration is specific for each value, moreover the error contribution comes from both the ADC and the OA. Another feature available when

dealing with arrays is the possibility to define a mask to redirect each value to the correct index of the output array.

$$I_{BP,i} = \left(\frac{X_{BP,i} \cdot S_{BP}}{G_{BP}} + O_{BP} \right) \cdot \frac{S_{PA,i}}{G_{PA,i}} + O_{PA,i}[A] \quad (3)$$

$$I_{FC} = \frac{X_{FC}}{G_{FC}} \cdot S_{FC} + O_{FC}[A] \quad (4)$$

On the other side, the abstraction layer, which does not communicate with the new hardware, gets the current values stored in the legacy PVs through the Channel Access (CA). The abstraction layer is used only for those diagnostics still controlled by the legacy control system.

Broken wires In BPs, a frequent problem is the presence of broken wires. Usually a broken wire is a disconnected wire, not measuring current, or a deformed wire touching one of the adjacent wires creating a short-circuit; in the latter case we have two adjacent broken wires showing saturated negative current and saturated positive current each. Given the array of the current values, user can select the index of the supposed broken wire and hide it. When there are broken wires a PV executes a C subroutine to restore the correct value.

Currently users can choose between two methods: the first sets broken wires current values equal to the mean value between the previous and the next valid wire; the second interpolates the array with a polynomial function of grade 7. With this grade, we saw a good approximation of the real values but other tests are still undergoing.

Handling control At the LNL we have different actuators controlled by specific IOCs: stepper motors, pneumatic motors and pneumatic pistons. Given the actuator type, the diagnostic IOC instantiates a set of standard PVs connected to the PVs of the IOC controlling that specific actuator. This way, users can move the correct instrument knowing nothing about the actuator details.

In addition to the interface with multiple IOCs, the handling logic converts the actuator position from its reference system (r.s.) to the beam line (or absolute) r.s. and vice-versa. This is achievable using a set of roto-translation matrices. More in details we assumed the detector instrument is mounted at the end of the actuator with a certain offset, along the X and Y axis, and a rotation angle along the XY plane. Similarly, the actuator is mounted over the flange with its set of offsets and angles. In the end, the flange is mounted with a specific distance from the center of the beam line and, depending on the box, it has a rotation angle. These three roto-translation matrices have the same shape described in Eq. (5) which represents a standard roto-translation along the z-axis. With these considerations, the correct parameters and the actuator position in its r.s., the logic returns the instrument accurate position represented in Eq. (6).

$$T = \begin{bmatrix} \cos(\theta) & -\sin(\theta) & O_x \\ \sin(\theta) & \cos(\theta) & O_y \\ 0 & 0 & 1 \end{bmatrix} \quad (5)$$

$$\begin{bmatrix} P_{xb} \\ P_{yb} \\ 1 \end{bmatrix} = T_{fb} \cdot T_{mf} \cdot T_{im} \cdot \begin{bmatrix} P_{xi} \\ P_{yi} \\ 1 \end{bmatrix} \quad (6)$$

On the other side, the abstraction layer, which does not know the alignment offsets, links the *insert* and *extract* commands to the legacy PVs not applying roto-translations. In those cases, the instruments position is nominal.

Collimators control Collimators (or slits) are a couple of metallic plates used to narrow the beam and the main parameters to control are the slot's center and aperture. In contrast to BPs and FCs, that can be only completely inserted or extracted they can reach different positions. There can be multiple types of collimators: two actuators, each with its plate, mounted over the same flange; two actuators, each with its plate, mounted over opposite flanges; a unique actuator, with both plates, controlling only the slot aperture size; a unique actuator, with both plates, controlling only the slot center position.

Considering that each slit has its own roto-translation logic, the control logic has an abstraction layer that, based on the collimators configuration, translates the set and read commands to show a common interface to the end user.

Graphical User Interface

A new CSS GUI, emulating the existing one, with additional features has been developed. The main page shows a list of the available transport elements such as triplets, dipoles and more. Chosen a specific item, users are redirected to the correct page. Since it is useful to monitor the measured current while changing a transport element parameters, diagnostics and transport element pages occupy only half of the horizontal screen size. Figure 6 shows the most important pages: the page showing the BP and the FC details and the page with the collimators position control. Other available pages are: the handling alignment parameters page, the broken wires page and the beam dynamics parameters page (with the parameters used to find the best beam trajectory).

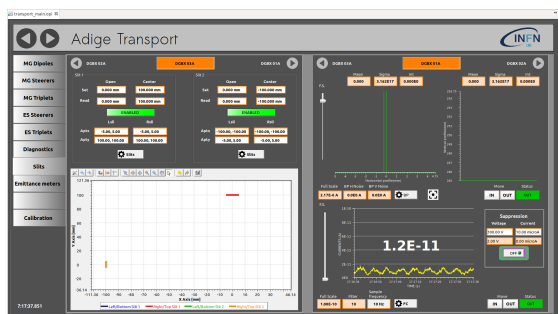


Figure 6: CSS based diagnostic GUI.

The BP section can show the vertical and the horizontal beam profile using two independent graphs or an intensity map; a slider allows to change the graphs full-scale and consequently the hardware gain. Each graph shows the correct position of each wire and the mean point of the current waveform. In addition the page shows the standard deviation and the total current measured by each profile. The FC section shows a graph with the current trend and a panel to set the suppression level. In both sections the page shows the actuator status and allows users to insert or extract the instrument. Another improvement is the presence of a set of parameters to graphically remove data noise and a set of buttons to open the actuator specific page.

The collimators page shows every slit system mounted in a specific diagnostic box. Two control modes exist: read and set the slot aperture and center; read and set the left and right slit position. Only collimators systems with two actuators have both the control modes, the others can control only the center or the aperture. At the page bottom there is an XY graphs showing the current position of each slit.

EMITTANCE METER

The emittance meter is based on two identical slit-grid type instruments that scan the beam in two orthogonal planes [7]. This method offers very clear results since the beam divergence is scanned directly and simplifies the calculations involved during the data analysis. The slit-grid instrument, consists of a grid (the detector), orthogonal to the beam, formed by 77 parallel wires, uniformly spaced by 1 mm and a plate (the collimator), parallel to the grid and placed 300 mm before the grid, with a slot of 0.3 mm aligned with the grid center. This solution allows for angular measurement in the range ± 60.0 mrad. A chassis holds the collimator and the detector and moves them together.

The electronics used to control the emittance meter acquisition and motion is the same used for the diagnostics. The main difference is that each emittance meter grid signal requires two pre-amplifier box channels and two controller channels. To reconstruct the correct signal the IOC combines together the signals belonging to those channels and then applies the conversion logic previously described. The motion control follows the same rules defined for the previous instruments.

Acquisition Procedure and Data Analysis

When the device is placed in the beam path, the slit selects the beam *slice* at that position and the grid reveals its divergence distribution. This way, the emittance measurement is performed by gradually inserting the slit across the beam path and measuring the divergence distribution on equally spaced rows, covering the whole beam area.

To perform this procedure the control system uses a python based Finite State Machine (FSM). It is a python script running in background using the *pysmilib* library [8]. This library helps creating event based FSMs, each running on a different thread, for EPICS control systems. The connection through

the CA to the desired PVs is provided by the well known library *pyepics*. The FSM checks its current state every time an input or output PV changes and, if the conditions allow it, the code of the specific state is executed. The library also provides timers for delayed operations which are largely used in this project to check if a motion has been completed.

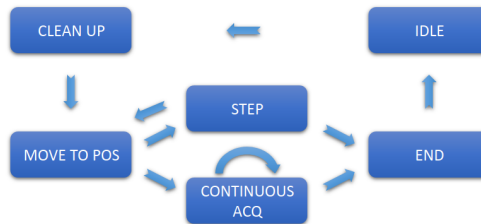


Figure 7: Python FSM to control the acquisition procedure and the ellipse calculation.

In the emittance meter FSM, as described in Fig. 7, the FSM remains in the idle state till the user starts the procedure. The procedure prevents the vertical and horizontal contemporaneous scanning that would lead to mechanical damages or inaccurate acquisitions. When the procedure starts, the FSM cleans up remaining values, moves the grid to the initial position and then starts the acquisition. There are two acquisition modes:

- **Step-by-step:** The FSM reads the current acquired by the grid and store the values in an array. It waits 0.5 s then goes to the next position, based on the number of steps and the ending position. It repeats these steps till the motor reaches the ending point.
- **Continuous:** The FSM moves the motor at constant speed till it reaches the ending position and constantly stores the values acquired by the grid into an array.

The resulting matrix contains, for each position, the array with the current values, acquired by the grid, included in the angular range defined at the beginning of the scan; those current values should return the emittance ellipse. At the end, the motor returns to the homing position (grid completely extracted) and the GUI, Fig. 8, shows the acquired matrix. From that GUI users can choose the acquisition mode (continuous or step by step), set the motion speed, the number of steps, the angles and positions range to consider when acquiring data and start or stop the acquisition procedure.

In some cases the ellipse estimation can be affected by errors since the presence of noise. For this reason the python script uses the scubeex-ghostbuster algorithm [9]. It is a recursive algorithm that estimates the ellipse (the beam current values at each position) and a threshold value (all values below the threshold will be considered noise and removed from the ellipse calculation) till it reaches an asymptote. At the end the *ghostbuster* routine removes the areas affected by the scattering of ions improving the emittance calculation. From the GUI, it is possible to change the threshold value and other parameters to manually find the best threshold value and the best emittance.

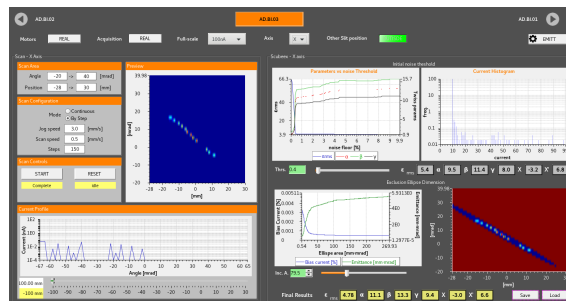


Figure 8: CSS based Emittance Meter GUI.

CONCLUSION

Our first test foresaw the installation of the new hardware and software to control to control one EM and two standard diagnostic boxes with one BP, one FC and one collimator systems each. This bench test was essential to test and improve the control logic. In fact these tests confirmed the improved quality of the hardware reading up to pA values, we successfully tested the EM FSM and operators gladly appreciate the new features making them the starting point for new high level functionalities. Subsequently we successfully started a different instance of the same IOC to test the translation layer for all the diagnostics currently mounted in ALPI. This was the first step for the general upgrade of the ALPI diagnostic control system. Confidants of the excellent results obtained from these tests, the next steps are the substitution of the legacy hardware in ALPI and the installation of the new SPES diagnostics.

REFERENCES

- [1] LNL site, accessed on Sep. 2021, <http://www.lnl.infn.it/index.php/en/>
- [2] G. Savarese *et al.*, “Design and development of the diagnostic control system for the SPES project”, Apr. 2019.
- [3] EPICS site accessed on Sep. 2021, <https://epics-controls.org/>
- [4] M. Bellato, A. Dainelli, and M. Poggi, “The beam diagnostic system of the ALPI post-accelerator”, in *Proc. EPAC’92*, Berlin, Germany, Mar. 1992, pg. 1085-1087.
- [5] M. Giacchini *et al.*, “Upgrade of the beam diagnostic system of ALPI-PIAVE accelerator’s complex at LNL”, in *Proc. PCAPAC’14*, Karlsruhe, Germany, Oct. 2014, paper WPO018, pp. 72–74.
- [6] D. Pedretti, “Design and Development of a Multi-Purpose Input Output Controller Board for the SPES Control System”, Ph.D. thesis, Università Degli Studi di Padova, 2018.
- [7] J. Montano *et al.*, “Off-line emittance measurements of the SPES ion source at LNL”, *Nucl. Instrum. Methods Phys. Res., Sect. A*, vol. 648, pp. 238-245, Aug. 2011. doi:10.1016/j.nima.2011.05.038
- [8] Pysmlib site, accessed on Sep. 2021, <https://darcato.github.io/pysmlib/docs/html/index.html>
- [9] L. Bellan *et al.*, “SCUBEEx-GHOSTBUSTER algorithm for ghost infested emittance measurements”, LNL-AR, Italy, 2015.